Brain Network Dynamics During Error Commission

Michael C. Stevens,[1,2]* Kent A. Kiehl,[3,4] Godfrey D. Pearlson,[1,2] and Vince D. Calhoun[1,2,3,5]

[1]*Olin Neuropsychiatry Research Center, Hartford, Connecticut*
[2]*Department of Psychiatry, Yale University School of Medicine, New Haven, Connecticut*
[3]*The MIND Institute, Albuquerque, New Mexico*
[4]*Department of Psychology, University of New Mexico, Albuquerque, New Mexico*
[5]*Department of Electrical and Computer Engineering, University of New Mexico, Albuquerque, New Mexico*

Abstract: Previous studies suggest that the anterior cingulate and other prefrontal brain regions might form a functionally-integrated error detection network in the human brain. This study examined whole brain functional connectivity to both correct and incorrect button presses using independent component analysis (ICA) of functional magnetic resonance imaging (fMRI) data collected from 25 adolescent and 25 adult healthy participants (ages 11–37) performing a visual Go/No-Go task. Correct responses engaged a network comprising left lateral prefrontal cortex, left postcentral gyrus/inferior parietal lobule, striatum, and left cerebellum. In contrast, a similar network was uniquely engaged during errors, but this network was not integrated with activity in regions believed to be engaged for higher-order cognitive control over behavior. A medial/dorsolateral prefrontal-parietal neural network responded to all No-Go stimuli, but with significantly greater activity to errors. ICA analyses also identified a third error-related circuit comprised of anterior temporal lobe, limbic, and pregenual cingulate cortices, possibly representing an affective response to errors. There were developmental differences in error-processing activity within many of these neural circuits, typically reflecting greater hemodynamic activation in adults. These findings characterize the spatial structure of neural networks underlying error commission and identify neurobiological differences between adolescents and adults. *Hum Brain Mapp 30:24–37, 2009.* © 2007 Wiley-Liss, Inc.

Key words: independent component analysis; network; error; brain; MRI; development; adolescent

INTRODUCTION

Successful behavior control requires the capacity to monitor ongoing actions to prevent responses when they would violate rules governing behavior. Older adolescents are able to respond faster and make fewer mistakes on Go/No-Go or similar tasks [Williams et al., 1999] compared with younger age groups. This suggests that there are normal maturational gains in cognitive control abilities that increase with age, consistent with the need to mediate increasing psychosocial and cognitive demands throughout maturation. Go/No-Go tasks require making manual responses to rapidly presented visual or auditory cues (i.e., 'Go' stimuli), but withholding responses in the presence of a different cue or signal ('No-Go' stimuli). In this para-

Contract grant sponsor: NIMH; Contract grant numbers: K23 MH070036, 1 R01 MH070539-01, 1 R01 MH071896-01; Contract grant sponsor: NIBIB; Contract grant numbers: R01 EB 000840, R01 EB005846; Contract grant sponsor: NIAAA; Contract grant numbers: RO1 AA015615, P50-AA12870; Contract grant sponsor: NIDA; Contract grant number: RO1 DA020709.

*Correspondence to: Michael C. Stevens, Ph.D., Olin Neuropsychiatry Research Center, Whitehall Building, The Institute of Living/Hartford Hospital, Hartford, Connecticut 06106, USA.
E-mail: msteven@harthosp.org

Received for publication 11 October 2006; Revised 10 July 2007; Accepted 14 August 2007

DOI: 10.1002/hbm.20478

Published online 2 November 2007 in Wiley InterScience (www.interscience.wiley.com).

digm, only two behavioral outcomes are possible for each 'No-Go' stimulus. One either will correctly withhold the planned response, or one will commit an error. One possibility for age-related performance gains is maturation of error monitoring abilities thought to be necessary for successful online performance maintenance [Botvinick et al., 2004; Ridderinkhof et al., 2004]. In humans, errors are believed to automatically engage a detection mechanism that compares a mental representation of the intended correct response to the actual response [Bernstein et al., 1995; Coles, 1998; Scheffers and Coles, 2000]. The exact cognitive mechanisms responsible for error recognition are debated [see Botvinick et al., 2004; Holroyd and Coles, 2002; Ullsperger and von Cramon, 2004; Yeung et al., 2004 for details on different hypotheses], but this specialized error processing system is thought to play a key role in integrating various neurocognitive systems, including neural response to outcome [Botvinick et al., 2004], use of error signals in learning [Holroyd and Coles, 2002], and performance adjustment [Ridderinkhof et al., 2004]. Therefore, there is great interest in better understanding how integrated brain systems respond to errors.

Brain activity associated with error processing can be observed as a response-locked error-related negativity (ERN) recorded during EEG [Gehring et al., 1990]. Although adolescents show smaller ERN amplitude than adults, ERN increases roughly linearly with age on several different tasks [Davies et al., 2004; Hogan et al., 2005; Ladouceur et al., 2004; Segalowitz and Davies, 2004], suggesting that there is maturation of the neural system that identifies different errors. In adults, brain electrical source analyses of the ERN [Coles, 1998; Luu et al., 2000], intracranial recordings [Bechtereva et al., 1990; Brazdil et al., 2002] and fMRI studies [see review by Ullsperger and von Cramon 2004] have localized the primary source of error-related brain activity to the rostral cingulate zone (RCZ) of anterior cingulate cortex [Kiehl et al., 2000]. These studies also report additional sources in bilateral anterior insulae, right parietal lobe regions, medial temporal lobe areas, basal ganglia, and the thalamus. No study has examined patterns of spatiotemporal correlation (i.e., 'functional connectivity') among brain regions engaged by correct 'Go' button presses or 'No-Go' errors, particularly with respect to identifying possible age-related differences. Brain regions are said to be 'functionally-connected' when they increase and decrease activity in conjunction. Because such coordinated activity often does not fit canonical models of hemodynamic change used in conventional fMRI timeseries, such analyses often miss identifying task-correlated brain activation. Data-driven methods that use hemodynamic data to identify functionally-integrated neural circuits provide the means to provide a more complete depiction of distributed networks engaged by task performance.

The current study had two main objectives. The first objective was to contrast functional neural networks associated with correct button presses versus errors to better understand the neurobiological substrates of human error-related cognitive processing. Specifically, our goal was to determine which subsets of brain regions identified by previous fMRI research formed functionally-integrated neural circuits during correct and incorrect button presses (i.e., Go 'hits' or No-Go errors) and to differentiate which networks were engaged by errors. Because there is ongoing debate regarding the exact cognitive mechanisms engaged for error detection, error monitoring, and error-based behavior correction, more complete and specific description of neural network function underlying error processing may ultimately help to clarify aspects of various theoretical proposals by identifying functional associations missed by traditional fMRI timeseries analysis. The second study objective was to assess whether these networks were more or less engaged from early adolescence to adulthood. Despite varying methods and results, fMRI studies of age differences in brain activity on Go/No-Go tasks show that adults typically have greater and more focal activity compared with youth [see review by Durston and Casey, 2006]. Some researchers have proposed that age-related performance gains may reflect a strengthening of anatomical connectivity between prefrontal cortex and posterior brain regions [Goldman-Rakic, 1987]. However, these increases in ability have not yet been linked to developmental changes in the function of any specific brain region or networks of brain regions. Evidence for increased functional connectivity during error processing across normal adolescent maturation would support proposals that age-related performance gains are related to continuing brain system specialization throughout development.

In this study, we used independent component analysis (ICA) to identify distinct, temporally coherent brain networks during performance of an event-related Go/No-Go fMRI task. We focused only on functionally-integrated network activity to correct and incorrect button presses, because results for correctly rejected No-Go stimuli involved with successful response inhibition are detailed in other work [Stevens et al., 2007b]. We hypothesized that errors would engage a network comprising anterior cingulate cortex and other previously identified neural sources of the ERN [Bechtereva et al., 1990; Brazdil et al., 2002; Coles, 1998; Luu et al., 2000; Ullsperger and von Cramon, 2004], including regions within anterior insulae, right parietal lobe, medial temporal lobe, basal ganglia, and thalamus. Consistent with the proposal that errors result from a breakdown of cognitive control [Ridderinkhof et al., 2004], we also predicted that neural network activity to No-Go failures would reflect a failure to integrate basal ganglia and lateral prefrontal cortex activity, which would be expected for accurate Go and No-Go performance [Bunge et al., 2001; Durston et al., 2002; Rubia et al., 2006]. In contrast, we hypothesized that correct 'hit' button presses to Go stimuli would be associated with functional connectivity among motor, basal ganglia, cerebellum and prefrontal and parietal lobe regions commonly engaged during deliberate goal-directed behavior. We also hypothesized that error-related neural networks would be increasingly

engaged with increasing age during error processing, which would be consistent with proposals that increased functional connectivity accompanies normal adolescent maturation.

METHODS

Participants

Participants were 50 healthy, screened, right-handed volunteers (64% male) between the ages of 11 and 37; mean (SD) = 19.9 (6.76). Participants were recruited via advertisements and word-of-mouth at the Olin Neuropsychiatry Research Center, Hartford, CT. Participants provided written informed consent in protocols approved by Hartford Hospital's Institutional Review Board. For legal minors, parents provided written permission and minors provided written assent. All research procedures were conducted in adherence to ethical standards required for human subjects protection.

Experimental Task

Participants were instructed to make a speeded button press with their right index finger to rapidly-presented visual 'X' (Go) stimuli, but to withhold response to pseudorandomly interspersed 'K' (No-Go) stimuli. To establish a prepotent response tendency, 85% of all stimuli were Go events. The Go/No-Go task consisted of frequent 'X' (P = 0.85) and infrequent 'K' stimuli presented at 3 × 5 visual degrees for 50 ms each. The minimum interstimulus interval was 1,000 ms. Intervals between 'K' stimuli were in the range of 10–15 s. Speed was emphasized over accuracy during a practice trial to ensure that participants would produce a sufficient number of commission errors for analysis. A custom visual and auditory presentation package was used to control stimuli presentation timing. The stimulus sequences were projected to the participant via a screen visible to participants in the MRI by rear-facing mirror attached to the head coil. Prior to beginning the task, each participant performed a practice trial to ensure understanding of the instructions and that responses were of sufficient speed to produce a sufficient number of errors for analysis. A commercially available MRI compatible fiber-optic response device (Lightwave Medical, Vancouver, BC) was used to acquire behavioral responses. Stimulus events and behavioral responses were recorded and monitored online using a separate computer. Hits and errors were defined as a response occurring within 1,000 ms of an 'X' or 'K' trial, respectively.

Imaging Parameters and Processing

Imaging was implemented on a Siemens Allegra 3T system located at the Olin Neuropsychiatry Research Center. Each participant's head was firmly secured using a custom head holder. Localizer images were acquired for use in prescribing the functional image volumes. The echo planar image (EPI) gradient-echo pulse sequence (TR/TE 1500/28 ms, flip angle 65°, FOV 24 × 24 cm^2, 64 × 64 matrix, 3.4 by 3.4 mm in plane resolution, 4-mm slice thickness, 1-mm gap, 29 slices) effectively covered the entire brain in 1.5 s. Head motion was restricted using a custom built cushion inside the head coil. The two stimulus runs each consisted of 294 time points, including a 9 s rest session at the beginning that was collected to allow for T_1 effects to stabilize. These initial six images were not included in any subsequent analyses. Functional images were reconstructed offline and each run was separately realigned using INRIAlign [Freire et al., 2002] as implemented in statistical parametric mapping (SPM2). Each participant's translation and rotation corrections were examined to ensure there was no excessive head motion. A mean functional image volume was constructed for each session from the realigned image volumes. This mean image volume was then used to determine parameters for spatial normalization into Montreal Neurological Institute standardized space employed in SPM2. The normalization parameters determined for the mean functional volume were then applied to the corresponding functional image volumes for each participant. These normalized data were corrected with a custom algorithm that used linear interpolation to remove variation in BOLD signal intensity because of slice acquisition temporal onset differences. Finally, the normalized functional images were smoothed with a 12-mm full width at half-maximum (FWHM) Gaussian filter.

Independent Component Analyses

Because ICA is relatively novel and not yet widely understood, we summarize our approach below. Our aim was to quantify the coupling between brain regions involved with correct and incorrect button presses on a Go/No-Go paradigm. To do this, we decomposed brain responses elicited by performance on a rapid, event-related visual Go/No-Go cognitive task into a series of spatially independent components, or modes, using ICA performed on fMRI timeseries data [Calhoun et al., 2001a,b]. ICA is a data-driven multivariate analysis method that identifies distinct groups of brain regions with the same temporal pattern of hemodynamic signal change. FMRI timeseries data for all 50 participants were first reduced through three principal component analysis (PCA) data reduction stages. At each stage, data were concatenated for further reduction. This method has been shown to be a useful approach to group ICA analysis [Calhoun et al., 2001b; Schmithorst and Holland, 2004]. The final PCA step included estimation of independent components representing spatiotemporal association algorithms described in detail in previous reports [Calhoun et al., 2001a; Calhoun et al., 2004]. In brief, this approach uses a neural network algorithm that attempts to minimize the mutual information of the network outputs [Bell and Sejnowski, 1995]. This ICA rotation was performed on the group of partici-

pants aggregate data to produce spatial maps and time-courses that represented both the spatial and temporal characteristics of each component 'network.' This was followed by a back reconstruction of single-subject time courses and spatial maps from the raw data using the group solution to accurately depict the participant-to-participant variability that existed in the data. The resulting single-subject time course amplitudes were then calibrated (scaled) using the raw data so that they reflected percent fMRI signal strength [Calhoun et al., 2001b] and could be compared across participants. The ICA methods are available in a Group ICA of FMRI Toolbox (GIFT v1.3c) implemented in Matlab (http://icatb.sourceforge.net).

In our dataset, the dimensionality of the data (number of components) was estimated using the minimum description length criteria tool built into GIFT, which suggested that at least 21 components were present in the data [Li et al., in press]. ICA then estimated 25 components. We identified those components whose temporal expression significantly correlated with explanatory variables based upon the experimental design. As in previous work [Stevens et al., 2007a,b], the R^2 association of each component's spatial map absolute values with *a priori* probabilistic masks of brain tissue (based on the MNI templates provided in SPM2) identified which components should be retained for further analysis. Inspection of the 17 components to be discarded showed they largely reflected eye movements, head motion, and cardiac-induced pulsatile artifact at the base of the brain. This approach misclassified two components that reflected valid brain activity in limited areas of cortex; these were not excluded. Therefore, a total of 10 components were retained for further consideration.

Examination of Component Temporal Dynamics

The time course analysis involved parameterizing the time courses to provide estimates of the association between component time course and experimental design. The conditions in the Go/No-Go experiment were represented using a canonical hemodynamic response model in SPM2. This SPM2 model separately represented hemodynamic response to hits, correct rejects, and 'false alarm' errors. These three event-classes were determined as per whether responses occurred within 1,000 ms post-stimulus. These analyses yielded R^2 values that represented the overall association of each condition in the experimental design to each component time course. The mean β-weights showing the relations of each component to experimental condition (hits, errors, and correct rejects) were examined using one-sample t tests against zero. Two components were associated with hits and four components were associated with errors (one component was associated with both hits and errors, for a total of five separate components). These five components were examined further for age effects using multivariate, repeated-measures regression models with age group as a covariate of interest. Follow-up t tests characterized which specific components showed a linear relationship with age. Statistical significance for all β-weight analyses was evaluated using the false discovery rate correction for multiple comparisons [Genovese et al., 2002].

Visualization of Spatial Components

Although we have already established that the components were significantly associated with correct or incorrect button presses using the convolution model above, we also created statistical parametric maps that quantify how the spatial structure of these components is conserved over subjects. Note that this model was not performed to make inferences about regionally specific effects across the whole sample. Rather, we were simply quantifying the spatial loading of each of the three components in relation to their variability over subjects. Error-processing and hit-processing maps were transformed to z-scores, incorporating a bias term to center each image's distribution of z-scores at zero. Because these ICA methods are known to produce individual session spatial maps with remarkable consistency to the group solution [Correa et al., 2007], z-score maps for the two sessions were averaged to produce one component map for each participant. These individual subject maps were entered into an SPM2 voxelwise one-sample t test in order to visualize which brain regions were statistically significant. Significance was evaluated using $P < 0.001$ family-wise error rate [Worsley et al., 1996] correction for searching the whole brain. Previous analyses employing these methods [Calhoun et al., 2004; Stevens et al., 2007a) indicate that stringent corrected statistical thresholds are appropriate for identifying which brain regions are incorporated into each independent component. Component spatial structure was visualized by color-coded component maps overlaid on axial slices of representative brain anatomy. Cortical surface renderings [Van Essen, et al., 2001] and figures depicting averaged ICA time course data were constructed for visualization of positive and negative signal change patterns. To visualize hemodynamic signal change in each neural network, ICA component time course data were averaged across conditions (hits or false alarm errors) separately for age-groups (11–18 vs. 19–37) to depict patterns of hemodynamic signal change (i.e., event-related averages).

Behavioral Analyses

Reaction time to hits and 'false alarm' errors were specified as a response occurring within 1,000 ms post-stimulus. Because there is some evidence for different reaction times before and following mistakes [Hester et al., 2004], hits were divided into correct 'Go' responses occurring before and after correctly rejected or error trials. A mean reaction time for all other 'Go' stimuli was calculated. The numbers of hits, correct rejects, and 'false alarms' also were quantified for each participant. Multivariate regression was used

TABLE I. Five components identified by ICA as associated with hits and errors during the Go/No-Go task

	Error average R^2	Hit average R^2	Mean (SD)			One-Sample t test P		
Figure 1 Color			Errors	Hits	Correct rejects	Errors	Hits	Correct rejects
Orange	0.007	0.058	−0.09 (0.96)	0.53 (1.24)	−0.08 (1.14)	ns	0.004	Ns
Red	0.024	0.049	1.06 (1.36)	0.26 (1.14)	0.31 (0.84)	<0.001	ns	0.012
Green	0.013	0.040	0.66 (1.23)	0.03 (1.04)	−0.13 (1.09)	<0.001	ns	Ns
Yellow	0.007	0.028	0.33 (0.78)	−0.18 (0.87)	−0.29 (0.79)	0.005	ns	0.011
Blue	0.007	0.040	−0.98 (1.76)	−1.19 (1.96)	−0.47 (1.74)	<0.001	<0.001	0.065[a]

The components are listed by corresponding color code depicted in Figures 1 and 2. The R^2 association to hits or errors to permit comparison of relative association to each condition. The subsequent three columns list the mean (SD) of regression coefficients indicating the strength of association between each component's ICA time course and each experimental condition. The table also lists the significance levels of the one-sample t-tests used to determine whether these loadings are statistically different from zero. Unless noted, all reported P values surpass FDR-corrected α 0.05.

[a] Trend level of significance.

to test for the presence of reaction time differences between adults and adolescents. Mixed model GLM tests examined differences between indices within the sample (e.g., false alarm versus 'Go' reaction time) and possible interactions with age.

RESULTS

Table I lists the components associated with error-processing and the one component uniquely associated with correct 'hits' identified in the ICA analysis and reports their association to each experimental condition of the Go/No-Go task. Brain regions within each component associated with hits are listed in Table II, along with the x, y, and z coordinates of the peak t score for each region. An illustration of hit-related components' spatial structures overlaid on a map of brain anatomy is shown in Figure 1A,B, separately color-coded for each component. Correct button presses uniquely engaged a left-hemisphere lateralized fronto-parietal-striatal-cerebellar network. In addition, hits engaged bilateral putamen activity increases with corresponding hemodynamic decreases primarily in ventromedial prefrontal cortex (Fig. 1B, Blue; Table II). Brain regions in the Blue component were engaged during all stimuli, albeit at a trend level of significance for No-Go correct rejects.

Brain regions associated with error-processing are listed in Table III and depicted in Figure 2A–C. Three functionally-connected networks were engaged during error processing. The Green component was uniquely engaged during No-Go errors. The Red and Yellow components were engaged both for errors and correctly inhibited No-Go trials, indicating that their engagement was not specific to error processing. Although the Yellow component responded to both correct and incorrect No-Go trials, brain regions within this component increased in amplitude during errors, but decreased activity for correctly inhibited No-Go successes. Finally, as mentioned above the Blue component was also engaged during error-processing.

Table IV lists the mean (SD) of β-weights representing how strongly each component was related to correct hits or incorrect button press errors, separately for adolescent and adult age groups. There was a significant multivariate linear effect of age group for β-weights measuring error-related functional connectivity ($F_{2,48}$ = 2.372, P = 0.046). Univariate tests show that there was a linear change in this association with age specifically for the Green, Yellow, and Blue components. Figure 3A–C shows the spatial extent of these components using cortical surface renderings of positive (Red-Yellow) and negative (Blue-Green) signal changes. It also plots event-related averages of the component time courses separately for groups of adolescents and adults defined by age median split to illustrate age differences. For all three components, the amplitude of signal change increased with age, suggesting that the significant relationship between task-association and age is related to hemodynamic amplitude increases with age. Univariate tests indicated that neither the Orange nor Blue hit-related components showed a significant age effect.

Table V lists the mean (SD) of behavioral performance measures for adolescents and adults. There were no differences between adults and adolescents in number of errors. This is consistent with instructions given to all participants to perform at their fastest speed and provides a comparable number of error-trials for age-group comparisons. Adults were generally faster than adolescents to respond to Go stimuli and during errors (Table V). No-Go errors were significantly faster than Go hits ($F_{1,48}$ = 17.233, P < .001), and this trial type difference did not differ by age group ($F_{1,48}$ = 0.917, ns).

DISCUSSION

This study used ICA to identify the spatial structure of neural networks engaged during correct and incorrect but-

TABLE II. List of brain regions within components significantly associated with correct hit button presses

Component	Regions	Brodmann areas	x	y	z	t_{49}
Orange	L superior frontal gyrus	8	−9	42	48	17.87
	L middle frontal gyrus	8	−42	8	51	21.33
	L middle frontal gyrus	9, 46	−51	27	24	21.99
	L middle frontal gyrus	10, 47	−45	42	−9	21.89
	R middle frontal gyrus	11, 47	42	42	−12	10.21
	L medial frontal gyrus	11	−6	−48	−18	9.48
	L postcentral gyrus	1, 2	−60	−27	39	6.63
	L inferior parietal lobule/supramarginal gyrus	40	−42	−48	51	22.63
	L superior parietal lobule/angular gyrus	7	−33	−66	48	24.11
	R inferior/superior parietal lobule	40	39	−66	48	9.60
	L cingulate gyrus	31	−6	−39	39	9.48
	L middle temporal gyrus	20, 21	−60	−39	−9	16.43
	R middle temporal gyrus	21	66	−36	−6	8.14
	L caudate		−15	9	6	13.99
	L putamen		−33	0	0	10.47
	R cerebellum		12	−84	−30	13.71
	R cerebellum		36	−78	−36	15.42
	↓ R superior/middle frontal gyri	9, 10	33	45	39	16.29
	↓ R medial frontal gyrus/anterior cingulate	9, 32	12	45	21	10.94
	↓ R pregenual cingulate	25	6	12	−9	10.85
	↓ R precuneus/posterior cingulate	7, 31	15	−69	30	10.39
	↓ L cerebellum		−39	−54	−39	9.71
Blue	L putamen/globus pallidus		−27	−6	−9	7.93
	R putamen		27	−6	−9	8.71
	↓ L middle frontal gyrus	10	−33	39	27	8.33
	↓ L medial/inferior frontal gyri, gyrus rectus	11, 25, 32, 47	−15	24	−18	26.19
	↓ L medial/inferior frontal gyri, gyrus rectus	11, 25, 32, 47	12	30	−21	23.91
	↓ L postcentral gyrus, inferior parietal lobule	1, 3, 40	−60	−27	45	8.65
	↓ L inferior temporal/fusiform gyri	20	−48	−24	−21	10.49
	↓ R inferior temporal/fusiform gyri		48	−24	−24	11.72
	↓ Cerebellum		−3	−45	−21	7.46

Columns depict component color (Fig. 1A,B), anatomical label and Brodmann areas, MNI coordinate for peak activation voxel in each brain region, and t-score from random effects analysis. Unless noted, regions show significant increases in hemodynamic activity. Regions noted ↓ show relative decreases in hemodynamic activity.

ton presses on a Go/No-Go task. The analysis found five distinct functional networks related to correct hits and errors. Correct button presses engaged a network that included left dorsolateral prefrontal cortex, left premotor cortex, bilateral ventrolateral prefrontal cortex, left postcentral gyrus, bilateral inferior parietal lobe, bilateral posterior middle temporal gyri, left caudate/putamen, and right cerebellum (Fig. 1A). Concurrently, there were hemodynamic decreases in this network in predominantly right hemisphere regions (i.e., right superior/middle frontal gyri, right medial frontal regions, right precuneus/posterior cingulate), and left cerebellum. This network shows functional integration of premotor/motor cortex, basal ganglia and cerebellum, which have been observed previously to be active to correct hits on this task [Kiehl et al., 2000]. Consistent with hypotheses, this motor system activation was functionally integrated with prefrontal and parietal regions frequently observed during goal-directed behavior involving motor attention and working memory.

Incorrect button presses engaged a different, but similar network comprising premotor, motor, and cerebellum regions of the motor execution system (Green; Figs. 2A and 3A). Consistent with hypotheses, brain activity accompanying the motor response was not positively coupled with activity in striatal brain regions typically associated with executive regulation of responses [Bunge et al., 2001; Durston et al., 2002; Rubia et al., 2006]. Nor was there evidence for activity in 'higher-order' regions engaged for successful response inhibition, such as right inferior frontal cortex or dorsolateral prefrontal cortex [Bunge et al., 2001; Durston et al., 2002; Rubia et al., 2006]. Instead, there were concurrent negative signal changes in some of these regions (i.e., left dorsolateral prefrontal cortex and caudate). This may reflect a breakdown of higher-order control on error trials. This interpretation is supported by the relative decrease of activity in regions in the Green component thought to be involved in motor planning and motor attention (i.e., pre-SMA, pre-PMd, and parietal cortex). In contrast to the RCZ and medial frontal activity observed to correct hits in the Orange network, motor cingulate in the caudal cingulate zone (CCZ) was instead engaged to errors. Comparative research and human neuroimaging studies have suggested a functional dissociation between the RCZ (thought to be involved primarily in action or conflict monitoring) and CCZ, which appears to be engaged by primarily by movement generation and control

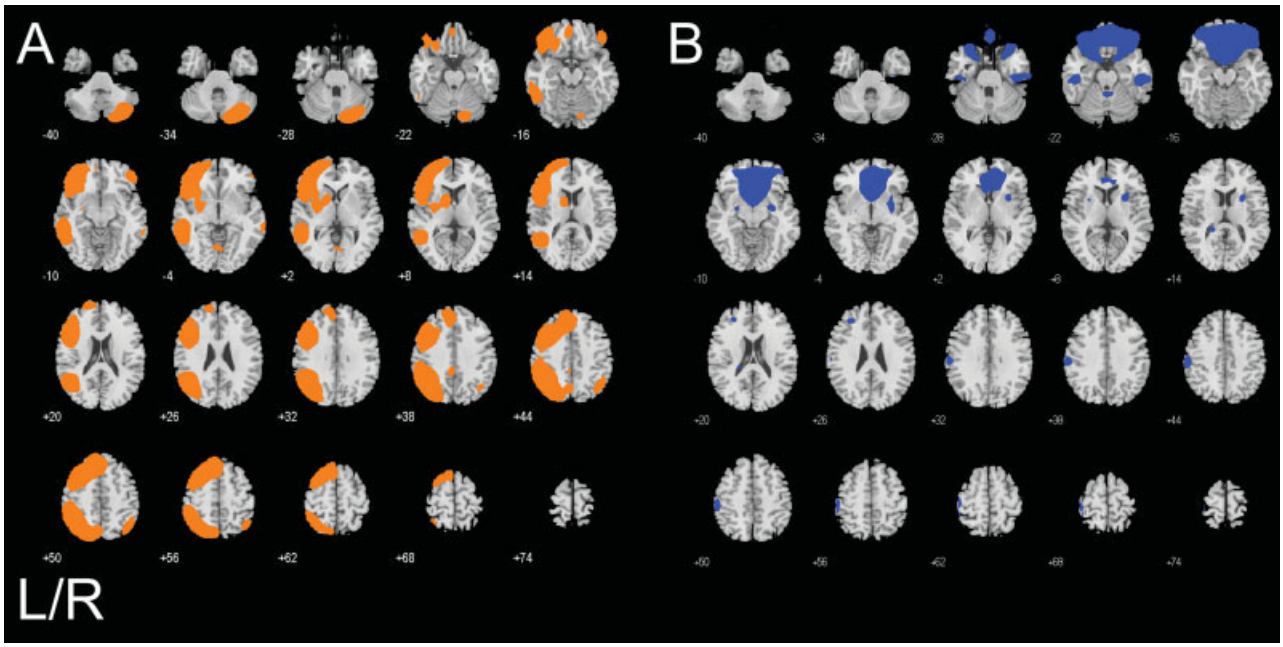

Figure 1.
Brain regions in each component associated with correct hit button presses. **A:** a motor-execution neural circuit integrated with frontal, parietal, and striatal regions (Orange), **B:** the 'default mode' neural network (Blue; also associated with errors, see Table I). Statistical results are thresholded at a low of $P < 0.001$, corrected for searching the whole brain.

[Picard and Strick, 2001]. Because CCZ activation was observed only in one of these two motor system circuits, it is possible that it represents specific aspects of error processing cognitive function, such as response conflict mediation [Hester et al., 2004]. Therefore, these results show a distinction between a motor circuit integrated with higher-order control brain regions engaged for successful hits versus a motor circuit not coupled with executive control neural systems during errors, instead showing activation of a region believed to process motor execution conflict.

The Green circuit included pronounced activation of bilateral superior/middle temporal gyri and cortex surrounding the central sulcus. Previous intracranial recording studies have found mesiotemporal lobe activity consistent with ERN [Bechtereva et al., 1990; Brazdil et al., 2002]. But because those previous studies did not use a task for which the motor response was prepotent, it is not clear whether the hemodynamic activity observed in this circuit represents the same phenomenon. One appealing functional interpretation of mesiotemporal activity is that it could represent internal speech [Ryding et al., 1996], a literal or figurative sub-vocal 'whoops!' response made to errors. This is consistent with the evidence for bilateral cerebellum activity in this component, which has been observed with such internal language [Ackermann et al., 2004]. Reasonable hypotheses include predictions that sub-vocal speech might signal the need for enhanced cognitive control, or might directly help to re-establish goal-directed response sets through linguistically-based neural pathways. Alternatively, this may reflect attention being diverted to auditory stimuli which causes distraction and performance error. However, these possibilities await further experimentation.

The component with greatest overall association to error trials (Fig. 2B; Red) showed activity within anterior cingulate (RCZ and CCZ), bilateral dorsolateral prefrontal cortex, bilateral insulae, and bilateral parietal lobe regions. Concurrently, there was negative signal change in temporal-parietal regions including bilateral fusiform gyri, left superior parietal lobule/precuneus, and right angular gyrus/precuneus. The prominent activation of the RCZ and other regions identified by previous source localization studies [Ullsperger and von Cramon, 2004] in this circuit makes it very likely that this neural network is related to the ERN observed in previous EEG studies. This conclusion also is consistent with our recent ERN/fMRI fusion study [Kiehl et al., in preparation], which explicitly links the ERN to hemodynamic activity in the anterior cingulate and other Red component regions. This convergence of results using multiple methods strengthens the already-identified role of RCZ anterior cingulate in error processing. The Red network likely depicts at least some of the brain regions observed in the ERN. These results also indicate that other regions could be related to the ERN,

TABLE III. List of brain regions within components significantly associated with No-Go errors

Component	Regions	Brodmann Areas	x	y	z	t_{49}
Red	Anterior cingulate gyrus (RCZ)	24, 32	3	33	27	19.99
	Anterior cingulate gyrus (CCZ)	24, 32	−6	9	42	20.30
	Cingulate gyrus	24	−6	−21	39	12.98
	L middle frontal/precentral gyri	9, 6	−42	0	42	10.08
	R middle frontal/precentral gyri	9, 6	51	12	30	8.71
	L superior/middle frontal gyri	9, 10	−30	45	30	19.19
	R superior/middle frontal gyri	9, 10	33	45	24	18.01
	L anterior insula	13, 47	−36	6	−3	19.21
	R anterior insula	13, 47	39	21	−3	17.44
	L inferior parietal lobule	40	−51	−39	39	10.16
	R inferior parietal lobule	40	57	−39	36	10.87
	Posterior cingulate/cuneus	30, 19	0	−66	0	8.24
	↓ L superior frontal gyrus	8	−33	21	60	8.36
	↓ R superior frontal gyrus	8	39	21	60	8.18
	↓ R precentral gyrus	4, 6	39	−21	63	10.80
	↓ medial frontal gyrus	11	−3	54	−15	9.42
	↓ L inferior/middle temporal gyrus	20, 21	−57	−12	−21	11.07
	↓ R inferior/middle temporal gyrus	20, 21	60	−3	−27	9.59
	↓ L parahippocampal/fusiform gyri	36, 37	−36	−36	−12	14.97
	↓ R parahippocampal/fusiform gyri	36, 37	36	−36	−15	15.29
	↓ L precuneus, inferior/superior parietal lobules, angular gyrus	7, 39, 40	−45	−72	42	15/55
	↓ R inferior parietal lobule, precuneus, angular gyrus	7, 19, 39	42	−72	51	13.18
Green	Cingulate gyrus (CCZ)	24, 32	−3	0	48	11.75
	L superior/middle frontal gyri	10, 9, 46	−36	60	21	7.93
	L precentral gyrus (PMd)	4, 6	−60	−15	39	18.76
	R precentral gyrus (PMd)	4, 6	63	−12	36	13.40
	L middle/inferior frontal gyri	11	−30	39	−24	7.99
	L postcentral gyrus	1, 2, 3	−57	−27	18	22.53
	L postcentral gyrus	1, 2, 3	−51	−18	60	13.98
	R postcentral gyrus	1, 2, 3	60	−24	18	19.28
	L transverse/superior temporal gyri	22, 41, 42	−54	−18	12	23.86
	R transverse/superior temporal gyri	22, 41, 42	63	−6	9	19.12
	L insula		−36	−18	12	21.75
	R insula		45	−12	12	23.02
	L cerebellum		−12	−60	−27	9.76
	R cerebellum		15	−60	−27	11.97
	L thalamus		−12	−18	3	12.72
	R thalamus		12	−15	3	12.17
	↓ L medial/superior frontal gyri (pre-SMA)	6, 8	−12	21	57	17.11
	↓ R medial/superior frontal gyri (pre-SMA)	6, 8	9	27	57	16.49
	↓ L middle frontal gyrus (pre-PMd)	6, 8	−30	0	39	12.00
	↓ R middle frontal gyrus (pre-PMd)	6, 8	30	6	42	13.62
	↓ L superior/inferior parietal lobules	7, 40	−27	−63	45	7.70
	↓ R superior/inferior parietal lobules	7, 40	33	−60	48	9.63
	↓ L middle temporal gyrus	21, 38	−45	9	−36	7.56
	↓ L caudate		−6	15	6	6.93
Yellow	Cingulate gyrus (pregenual)	25	3	9	−9	11.93
	Medial frontal gyrus	9, 10	−3	48	15	7.76
	L angular/supramarginal gyri	40	−54	−60	33	9.21
	R inferior parietal lobule, supramarginal gyrus	40	57	−54	24	8.31
	R superior/middle temporal gyri, parahippocampal gyrus, inferior frontal gyrus, amygdala, hippocampus, insula	21, 22, 38, 13, 47	−36	18	−15	27.99
	L superior/middle temporal gyri, parahippocampal gyrus, inferior frontal gyrus, amygdala, hippocampus, insula	21, 22, 38, 13, 47	51	6	−15	25.64
	L cerebellum		−24	−54	−21	9.51
	↓ L middle frontal gyrus	9, 46	−51	33	33	8.74
	↓ R middle frontal gyrus	9, 46	48	45	30	8.54
	↓ L precentral/inferior frontal gyri	6, 9	−51	3	33	12.01
	↓ R precentral/inferior frontal gyri	6, 9	54	−15	30	8.48
	↓ L postcentral gyrus	3	−57	−18	36	10.31
	↓ L middle/inferior frontal gyri	46	−36	33	15	9.57
	↓ L posterior cingulate	30, 31	−9	−57	18	8.51
	↓ R posterior cingulate	30, 31	9	−54	18	8.18
	↓ L putamen		−21	−6	6	8.88
	↓ R putamen		24	−6	6	7.21
	↓ Midbrain		6	−21	−6	9.44

Columns depict component color (Figure 2A-C), anatomical label and Brodmann areas, MNI coordinate for peak activation voxel in each brain region, and t-score from random effects analysis. Unless noted, regions show significant increases in hemodynamic activity. Regions noted ↓ show relative decreases in hemodynamic activity.

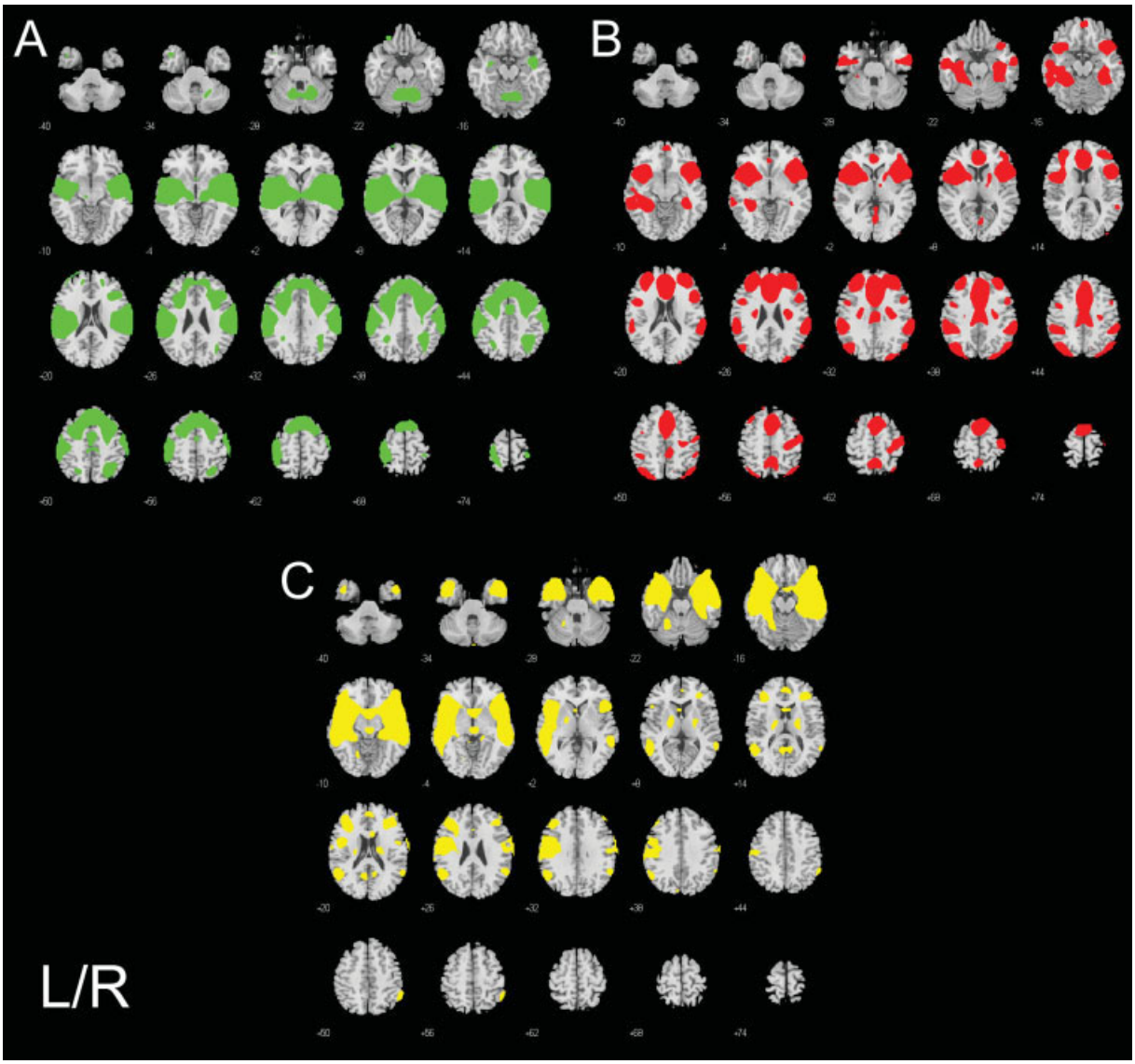

Figure 2.

Brain regions in each component associated with errors. **A:** a motor-execution neural circuit showing absent or decreased activity in brain regions engaged for higher-order control (Green), **B:** a low-probability stimulus processing functional circuit that has a greater response amplitude to errors (Red), **C:** the pregenual cingulate-temporal lobe network possibly reflecting an affective response to errors (Yellow). Statistical results are thresholded at a low of $P < 0.001$, corrected for searching the whole brain.

including dorsolateral prefrontal cortex and other parietal lobe and temporal lobe cortex regions. It is relevant to note that scalp-recorded response-locked ERNs likely reflect a combination of different frontomedial sources. Previous source localization studies did not differentiate brain regions with activation increases compared with those that decrease. The current results show that this combination includes several anatomically proximate regions—CCZ activity increases (also seen in the Green error-related network) and pre-SMA/pre-PMd cortex activity decreases, plus RCZ and other regions' activity increases. Thus, it is important to carefully consider the possible implications of this mixture of sources when ascribing functional or cognitive significance of scalp-recorded ERPs to the function of particular brain regions.

We also found that this Red circuit was engaged for all No-Go stimuli – regardless of whether the stimulus was classified correctly or whether a false alarm error was

TABLE IV. Regression coefficient mean (SD) for β-weights representing task-association separately adolescents and adults and results of univariate linear tests of age

Component	Time Course Coefficient Mean (SD)		Linear Effect of Age[a] *P*
	Adolescents	Adults	
Hits			
Orange	0.52 (1.42)	−1.53 (1.94)	ns
Blue	−0.39 (1.24)	−1.98 (2.24)	ns
Errors			
Red	0.75 (1.38)	1.36 (1.29)	ns
Green	0.32 (0.71)	0.99 (1.53)	0.012
Yellow	0.19 (0.96)	0.46 (0.54)	0.052
Blue	−0.42 (1.38)	−1.53 (1.94)	0.044

[a] Uncorrected level of significance following significant multivariate GLM.

made. This suggests that activity in this network is not specific to errors, but may instead reflect neural processing related to low-probability stimulus processing. Importantly, activity in this Red network was augmented by error trials, such that errors elicited significantly greater signal change in the network than did correctly inhibited trials. Therefore, it is possible that error detection might be directly related to simple performance monitoring neural activity, with errors marked by greater engagement of the Red circuit. Recent proposals suggest error-related activation of anterior cingulate follows dopaminergic signaling of suboptimal outcome using information provided by other prefrontal and parietal brain regions [Holroyd and Coles, 2002], perhaps to signal subsequent performance adjustment, as some have suggested [Ridderinkhof et al., 2004; Rushworth et al., 2004]. Indeed, this Red circuit was more strongly associated with correct No-Go trials than Go hits, and most strongly associated with error trials. This is consistent with predictions of conflict detection theory [Botvinick et al., 2004].

The existence of multiple error-related neural networks is consistent with previous proposals [Garavan et al., 2003; Mathalon et al., 2003; Ullsperger and von Cramon, 2001) and suggests that each network might primarily underlie a different cognitive function. Both the Green and Red circuits included CCZ activation, raising the possibility that activity in one circuit might directly influence the other. In the absence of additional information at this time, we speculate that the functionally-integrated activity observed in the Green circuit might serve to engage CCZ during conflict monitoring, thereby contributing to activation of the Red RCZ-dominated network in the service of dopaminergically-guided performance adjustment. Future studies should examine the causal relationships between brain activity in these areas during errors, particularly in the context of various experimental factors known to modulate ERN amplitude, such as the size of the error [Bernstein et al., 1995], amount of preresponse conflict [Botvinick et al., 2004], judgments of response accuracy [Scheffers and Coles, 2000], and reward likelihood [Ridderinkhof et al., 2004; Ullsperger and von Cramon, 2004]. Such research could shed light on the exact functional significance of each network in error-related cognitive processing.

In response to all No-Go stimuli regardless of performance, the third error-related component (Yellow; Figs.2C and 3B) showed functional integration of pregenual anterior cingulate (BA 25) with regions within bilateral inferior frontotemporal cortices. This connectivity is consistent with comparative studies that find anatomical connections among pregenual cingulate, ventral temporal pole regions, and insular cortices [Kondo et al., 2003]. The pregenual cingulate area has been linked to processing affective information related to errors [Kiehl et al., 2000], suggesting that activity in this neural network may also reflect an affective response to errors [Bush et al., 2000]. Consistent with this interpretation, this circuit includes bilateral amygdala activation, which likely contributes affective salience to No-Go target stimuli [Holroyd and Coles, 2002]. Activity in these frontotemporal areas has been linked to internally-generated emotional response [Reiman et al., 1997], awareness of errors [Hester et al., 2005], and self-referential thinking [Vogeley et al., 2001], suggesting these regions may underlie awareness of and emotional reaction to errors. These attributes also have been ascribed to electrophysiological measures of positive signal change that occurs after errors (i.e., the 'Pe' ERP or 'error positivity') [van Veen and Carter, 2006], which raises the interesting possibility that this circuit may reflect an anatomical basis of this ERP. Indeed, there is some preliminary support for this notion from Pe source localization research [O'Connell et al., 2007; Van Boxtel et al., 2005; Van Veen and Carter, 2002). Importantly, No-Go stimuli performance outcome altered the direction of signal change in these brain regions. As indicated in Table I by the positive β-weight loading for this component, No-Go errors were associated with activated cingulate and frontotemporal regions. In contrast, negative β-weights for the other trial types indicate that integrated activity decreased in these regions during successful response inhibition or during Go hits. The outcome-dependent modulation of activity in these regions possibly reflects the presence or absence of a negative emotional response. Notably, as activity increased in these limbic and paralimbic regions, it decreased in dorsolateral prefrontal cortex and bilateral putamen. Activity in these latter brain regions is observed during trial-and-error based learning [Holroyd and Coles, 2002]. This functional coupling suggests a key component of such learning may be an affective response to errors. Specifically, affective responses might signal the failure to reinforce stimulus-action-reward associations. This possibility is supported by recent studies of brain activity during associative learning that found reduced activity in putamen in nonre-

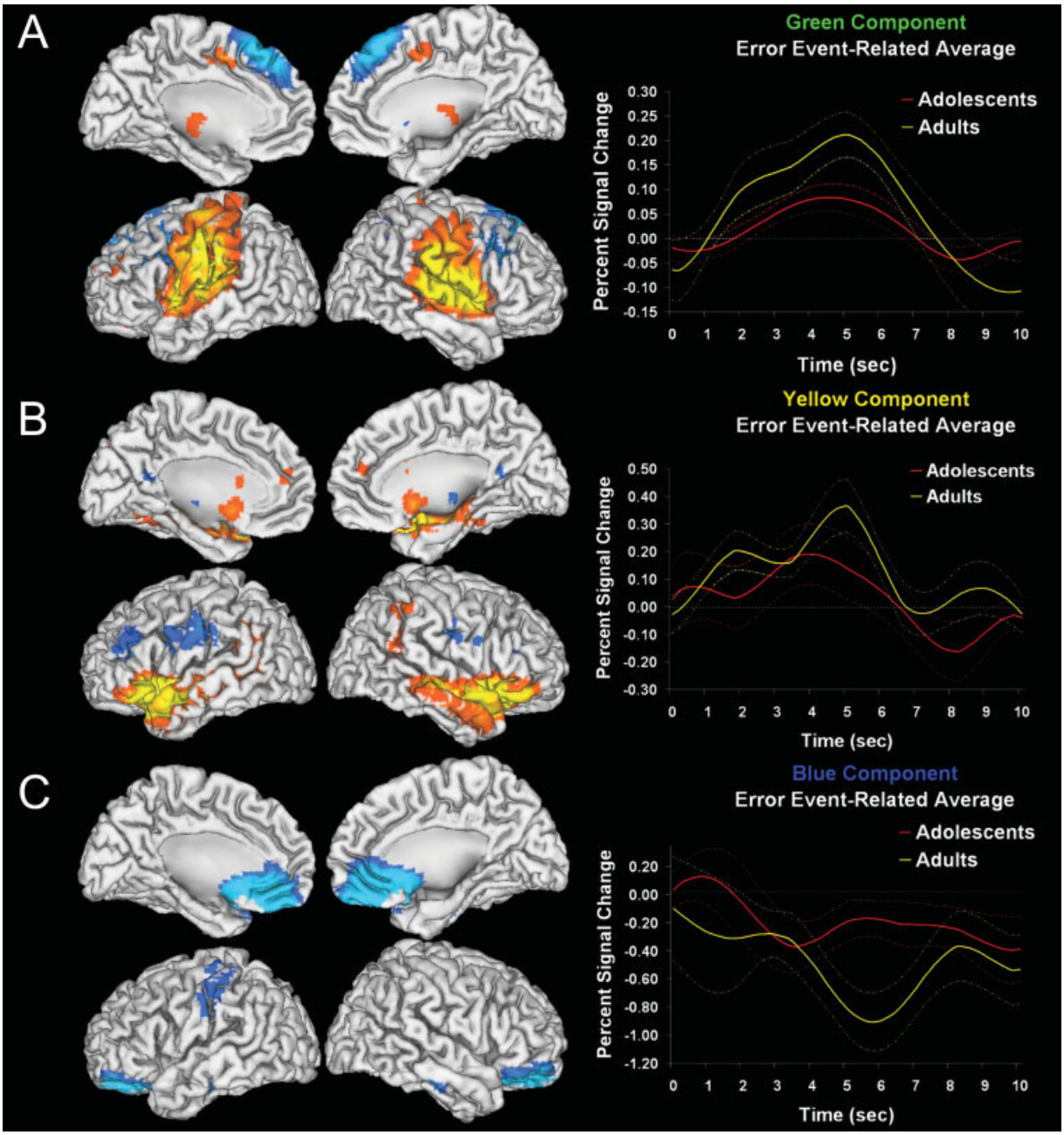

Figure 3.

Cortical surface renderings of positive (orange-yellow) and negative (blue-aqua) signal change in each component. Statistical results are thresholded at a low of $P < 0.001$, corrected for searching the whole brain. Each component hemodynamic time course is averaged over errors separately for adolescent and adult age groups to illustrate significant linear effects of age (dashed lines indicate standard error of measurement). **A–C:** corresponds with the green, yellow, and blue components, respectively.

ward trials [Haruno and Kawato, 2006], which presumably are interpreted by the brain as 'errors.'

The final component (Blue; Figs. 1B and 3C) showed relative signal decreases in medial orbitofrontal gyrus, left postcentral gyrus, and cerebellum during processing of all stimuli. Orbitofrontal cortex activation is associated with representing motivationally salient and reinforcing information in order to monitor whether outcomes meet expect-

TABLE V. Mean (SD) of 'No-Go' errors and reaction time (ms) to 'Go' and 'No-Go' responses for adolescents and adults. The table also lists t test results comparing adolescent and adult performance

			Age t test	
	Adolescents	Adults	t_{48}	P
Number of false alarms	36.1 (12.54)	36.2 (12.29)	−0.0384	ns
False alarm reaction time	365.1 (41.09)	329.7 (27.31)	3.593	0.001
Average 'Go' reaction time[a]	393.5 (49.21)	367.3 (32.99)	2.211	0.032

[a] Computed for 'Go' trials that did not immediately precede or follow any 'No-Go' stimulus.

ations [Elliott and Deakin, 2005]. Previous studies have interpreted similar task-induced signal decreases as reflecting resource allocation during cognitively demanding tasks, possibly reflecting decreased evaluation of extraneous sensory stimuli [Gusnard and Raichle, 2001; Raichle et al., 2001]. Concurrently, there were signal increases in bilateral putamen. The connectivity found in this circuit is consistent with direct dopaminergic connections between medial orbitofrontal cortex and the striatum [Haber et al., 1995]. Therefore, this circuit may also monitor performance, balancing processing resources with ongoing performance via interconnection of orbitofrontal cortex, the striatum, and other cortical and cerebellar regions.

Age Differences in Neural Network Function

Linear regression analyses found no differences between adolescents and adults in the engagement of the hit-related (Orange) or one of the error-related (Red) neural circuits, suggesting that some of the neural networks engaged by correct and incorrect Go/No-Go performance are functionally mature by adolescence. This is interesting in the context of previous reports that the hemodynamic response during Go/No-Go performance generally increases between adolescence and adulthood in numerous brain regions [Booth et al., 2003; Bunge et al., 2002; Durston et al., 2002; Rubia et al., 2000, 2006; Tamm et al., 2002]. All these previous studies focused on response-inhibition by contrasting successful No-Go related activation to hits or similar control conditions. Therefore, it is important to have evidence that hemodynamic activity during correct hit conditions used as baselines does not appear to change between adolescence and adulthood in the No-Go task context. The observation that there were no age-related hemodynamic response amplitude gains in the Red network also has important implications. The Red network had prominent engagement of the RCZ in anterior cingulate cortex. As described earlier, this brain region has been observed to be frequently engaged for error processing in previous neuroimaging studies [Ullsperger and von Cramon, 2004], has been linked to the ERN [Coles, 1998; Luu et al., 2000], and is thought to play a key role in error monitoring and perhaps signaling subsequent performance adjustment. The current results suggest that the neural substrates of these cognitive abilities may be neurobiologically mature by adolescence. This finding stands in contrast to previous ERP studies that find ERN increases with age [Davies et al., 2004; Hogan et al., 2005; Ladouceur et al., 2004; Segalowitz and Davies, 2004]. However, the discrepancy may reflect the fact that the ERN is calculated from scalp-recorded electrical activity, possibly averaging signals from numerous specific brain regions other than just the Red circuit identified here.

The relative engagement of the other three error-related components increased linearly with age (Table III and Fig. 3). Assuming an accurate functional interpretation of these three circuits, adults' errors might reflect greater activation of planned responses and/or breakdown of cognitive control (Green). Errors might induce a weaker affective response in adolescents, or these regions do not yet have the degree of functional specialization as in adulthood (Yellow). During both hits and errors, adolescents might engage less processing resources (Blue). Experience-based functional specialization and ongoing brain maturation are reasons commonly advanced to explain such changes in brain function [Goldman-Rakic, 1987; Pollak, 2005]. Changes in neural network response amplitude may represent a fine-tuning of neural systems or similar neurodevelopmental changes, such as increasing reliance on new brain regions, reduced involvement of others, or shifts in cognitive strategy [Durston and Casey, 2006]. However, these possible explanations are as yet circumstantial, because studies have not yet directly linked anatomical changes throughout maturation to neural network function.

CONCLUSIONS

This study used a multivariate analysis technique to identify and characterize several integrated neural networks functioning during correct and incorrect performance of an fMRI Go/No-Go task in healthy adolescents and adults. Many of the brain regions previously identified as active during correct hits or errors are here shown to be functionally coupled, indicating that subsets of these regions form integrated circuits with plausibly different functional roles. The current results suggest several key conclusions that help advance our understanding of cogni-

tive processes that underlie error processing. First, although both correct and incorrect button presses engage a similar motor network, the neural circuit activity underlying errors does not functionally couple the motor system to brain regions believed to be important for higher-order cognitive control (i.e., prefrontal, parietal, and striatal regions). This circuit is an ideal candidate to explore in order to clarify mechanisms through which rash or impulsive decision-making is made, as presumably this network might be preferentially engaged in psychiatric illnesses such as ADHD, Conduct Disorder, or other 'disinhibited' disorders. Second, there is evidence for multiple error-processing networks in the human brain. Error processing engages the conjoint function of numerous frontal (particularly anterior cingulate) and parietal lobe regions. Although these regions also are engaged during successful performance, the degree of activation in these regions is modulated when an error occurs. These findings set the stage for future studies and reexamination of current fMRI data to determine how experimental manipulation of these circuit's activity by degree of conflict, types of error, or motivational factors influence brain connectivity. We also found evidence for an error-related network whose function might be to process the affective reaction to committing an error. Finally, adults showed greater response amplitude in several error-related circuits compared with adolescents. This suggests that normal maturation involves greater responsiveness of key brain networks to errors. Future research should identify and characterize the development of which specific neural mechanisms and performance contexts lead to greater hemodynamic response in adulthood.

REFERENCES

Ackermann H, Mathiak K, Ivry RB (2004): Temporal organization of "internal speech" as a basis for cerebellar modulation of cognitive functions. Behav Cogn Neurosci Rev 3:14–22.

Bechtereva NP, Kropotov JD, Ponomarev VA, Etlinger SC (1990): In search of cerebral error detectors. Int J Psychophysiol 8:261–273.

Bell AJ, Sejnowski TJ (1995): An information-maximization approach to blind separation and blind deconvolution. Neural Comput 7:1129–1159.

Bernstein PS, Scheffers MK, Coles MGH (1995): "Where did I go wrong?" A psychophysiological analysis of error detection. J Exp Psychol Hum Percept Perform 21:1312–1322.

Booth JR, Burman DD, Meyer JR, Lei Z, Trommer BL, Davenport ND, Li W, Parrish TB, Gitelman DR, Mesulam MM (2003): Neural development of selective attention and response inhibition. Neuroimage 20:737–751.

Botvinick MM, Cohen JD, Carter CS (2004): Conflict monitoring and anterior cingulate cortex: An update. Trends Cogn Sci 8:539–546.

Brazdil M, Roman R, Falkenstein M, Daniel P, Jurak P, Rektor I (2002): Error processing—Evidence from intracerebral ERP recordings. Exp Brain Res 146:460–466.

Bunge SA, Ochsner KN, Desmond JE, Glover GH, Gabrieli JD (2001): Prefrontal regions involved in keeping information in and out of mind. Brain 124:2074–2086.

Bunge SA, Dudukovic NM, Thomason ME, Vaidya CJ, Gabrieli JD (2002): Immature frontal lobe contributions to cognitive control in children: Evidence from fMRI. Neuron 33:301–311.

Bush G, Luu P, Posner MI (2000): Cognitive and emotional influences in anterior cingulate cortex. Trends Cogn Sci 4:215–222.

Calhoun VD, Adali T, McGinty VB, Pekar JJ, Watson TD, Pearlson GD (2001a): fMRI activation in a visual-perception task: Network of areas detected using the general linear model and independent components analysis. Neuroimage 14:1080–1088.

Calhoun VD, Adali T, Pearlson GD, Pekar JJ (2001b): A method for making group inferences from functional MRI data using independent component analysis. Hum Brain Mapp 14:140–151.

Calhoun VD, Pekar JJ, Pearlson GD (2004): Alcohol intoxication effects on simulated driving: Exploring alcohol-dose effects on brain activation using functional MRI. Neuropsychopharmacology 29:2097–2117.

Coles MGH (1998): Preparation, sensory-motor interaction, response evaluation, and event-related brain potentials. Cahiers de Psychologie Cogn/Curr Psychol Cogn 17:737–747.

Correa N, Adali T, Calhoun VD (2007): Performance of blind source separation algorithms for fMRI analysis using a group ICA method. Magn Reson Imaging 25:684–694.

Davies PL, Segalowitz SJ, Gavin WJ (2004): Development of error-monitoring event-related potentials in adolescents. Ann NY Acad Sci 1021:324–328.

Durston S, Casey BJ (2006): What have we learned about cognitive development from neuroimaging? Neuropsychologia 44:2149–2157.

Durston S, Thomas KM, Yang Y, Ulug AM, Zimmerman RD, Casey B (2002): A neural basis for the development of inhibitory control. Dev Sci 5:F9–F16.

Elliott R, Deakin B (2005): Role of the orbitofrontal cortex in reinforcement processing and inhibitory control: Evidence from functional magnetic resonance imaging studies in healthy human subjects. Int Rev Neurobiol 65:89–116.

Freire L, Roche A, Mangin JF (2002): What is the best similarity measure for motion correction in fMRI time series? IEEE Trans Med Imaging 21:470–484.

Garavan H, Ross TJ, Kaufman J, Stein EA (2003): A midline dissociation between error-processing and response-conflict monitoring. Neuroimage 20:1132–1139.

Gehring WJ, Coles MGH, Meyer DE (1990): The error-related negativity: An event-related brain potential accompanying errors. Psychophysiology 27:S43.

Genovese CR, Lazar NA, Nichols T (2002): Thresholding of statistical maps in functional neuroimaging using the false discovery rate. Neuroimage 15:870–878.

Goldman-Rakic PS (1987): Development of cortical circuitry and cognitive function. Child Dev 58:601–622.

Gusnard DA, Raichle ME (2001): Searching for a baseline: Functional imaging and the resting human brain. Nat Rev Neurosci 2:685–694.

Haber SN, Kunishio K, Mizobuchi M, Lynd-Balta E (1995): The orbital and medial prefrontal circuit through the primate basal ganglia. J Neurosci 15 (7 Part 1):4851–4867.

Haruno M, Kawato M (2006): Different neural correlates of reward expectation and reward expectation error in the putamen and caudate nucleus during stimulus-action-reward association learning. J Neurophysiol 95:948–959.

Hester RL, Murphy K, Foxe JJ, Foxe DM, Javitt DC, Garavan H (2004): Predicting success: Patterns of cortical activation and deactivation prior to response inhibition. J Cogn Neurosci 16:776–785.

Hester R, Foxe JJ, Molholm S, Shpaner M, Garavan H (2005): Neural mechanisms involved in error processing: A comparison of errors made with and without awareness. Neuroimage 27:602–608.

Hogan AM, Vargha-Khadem F, Kirkham FJ, Baldeweg T (2005): Maturation of action monitoring from adolescence to adulthood: An ERP study. Dev Sci 8:525–534.

Holroyd CB, Coles MG (2002): The neural basis of human error processing: Reinforcement learning, dopamine, and the error-related negativity. Psychol Rev 109:679–709.

Kiehl KA, Stevens MC, Pearlson GD, Calhoun VD (in preparation). Dissecting emotion and cognition during error monitoring: Fusion of electrophysiological and hemodynamic data.

Kiehl KA, Liddle PF, Hopfinger JB (2000): Error processing and the rostral anterior cingulate: An event-related fMRI study. Psychophysiology 37:216–223.

Kondo H, Saleem KS, Price JL (2003): Differential connections of the temporal pole with the orbital and medial prefrontal networks in macaque monkeys. J Comp Neurol 465:499–523.

Ladouceur CD, Dahl RE, Carter CS (2004): ERP correlates of action monitoring in adolescence. Ann NY Acad Sci 1021:329–336.

Li YO, Adali T, Calhoun VD (2007): Estimating the number of independent components for functional magnetic resonance imaging data. Hum Brain Mapp. 2007 Feb 1; [Epub ahead of print].

Luu P, Flaisch T, Tucker DM (2000): Medial frontal cortex in action monitoring. J Neurosci 20:464–469.

Mathalon DH, Whitfield SL, Ford JM (2003): Anatomy of an error: ERP and fMRI. Biol Psychol 64:119–141.

O'Connell RG, Dockree PM, Bellgrove MA, Kelly SP, Hester R, Garavan H, Robertson IH, Foxe JJ (2007): The role of cingulate cortex in the detection of errors with and without awareness: A high-density electrical mapping study. Eur J Neurosci 25:2571–2579.

Picard N, Strick PL (2001): Imaging the premotor areas. Curr Opin Neurobiol 11:663–672.

Pollak SD (2005): Early adversity and mechanisms of plasticity: Integrating affective neuroscience with developmental approaches to psychopathology. Dev Psychopathol 17:735–752.

Raichle ME, MacLeod AM, Snyder AZ, Powers WJ, Gusnard DA, Shulman GL.(2001): A default mode of brain function. Proc Natl Acad Sci USA 98:676–682.

Reiman EM, Lane RD, Ahern GL, Schwartz GE, Davidson RJ, Friston KJ, Yun LS, Chen K (1997): Neuroanatomical correlates of externally and internally generated human emotion. Am J Psychiatry 154:918–925.

Ridderinkhof KR, Ullsperger M, Crone EA, Nieuwenhuis S (2004): The role of the medial frontal cortex in cognitive control. Science 306:443–447.

Rubia K, Overmeyer S, Taylor E, Brammer M, Williams SC, Simmons A, Andrew C, Bullmore ET (2000): Functional frontalisation with age: Mapping neurodevelopmental trajectories with fMRI. Neurosci Biobehav Rev 24:13–19.

Rubia K, Smith AB, Woolley J, Nosarti C, Heyman I, Taylor E, Brammer M (2006): Progressive increase of frontostriatal brain activation from childhood to adulthood during event-related tasks of cognitive control. Hum Brain Mapp 27:973–993.

Rushworth MF, Walton ME, Kennerley SW, Bannerman DM (2004): Action sets and decisions in the medial frontal cortex. Trends Cogn Sci 8:410–417.

Ryding E, Bradvik B, Ingvar DH (1996): Silent speech activates prefrontal cortical regions asymmetrically, as well as speech-related areas in the dominant hemisphere. Brain Lang 52:435–451.

Scheffers MK, Coles MG.(2000): Performance monitoring in a confusing world: Error-related brain activity, judgments of response accuracy, and types of errors. J Exp Psychol Hum Percept Perform 26:141–151.

Schmithorst VJ, Holland SK (2004): Comparison of three methods for generating group statistical inferences from independent component analysis of functional magnetic resonance imaging data. J Magn Reson Imaging 19:365–368.

Segalowitz SJ, Davies PL (2004): Charting the maturation of the frontal lobe: An electrophysiological strategy. Brain Cogn 55:116–133.

Stevens MC, Kiehl KA, Pearlson GD, Calhoun VD (2007a): Functional neural circuits for mental timekeeping. Hum Brain Mapp 28:394–408.

Stevens MC, Kiehl KA, Pearlson GD, Calhoun VD (2007b): Functional neural networks underlying response inhibition in adolescents and adults. Behav Brain Res 181:12–22.

Tamm L, Menon V, Reiss AL (2002): Maturation of brain function associated with response inhibition. J Am Acad Child Adolesc Psychiatry 41:1231–1238.

Ullsperger M, von Cramon DY (2001): Subprocesses of performance monitoring: A dissociation of error processing and response competition revealed by event-related fMRI and ERPs. Neuroimage 14:1387–1401.

Ullsperger M, von Cramon DY (2004): Neuroimaging of performance monitoring: Error detection and beyond. Cortex 40:593–604.

Van Boxtel G, Van der Molen M, Jennings J (2005): Differential involvement of the anterior cingulate cortex in performance monitoring during a stop-signal task. J Psychophysiol 19:1–10.

Van Essen DC, Drury HA, Dickson J, Harwell J, Hanlon D, Anderson CH (2001): An integrated software suite for surface-based analyses of cerebral cortex. J Am Med Inform Assoc 8:443–459.

Van Veen V, Carter CS (2002): The timing of action-monitoring processes in the anterior cingulate cortex. J Cogn Neurosci 14:593–602.

van Veen V, Carter CS (2006): Error detection, correction, and prevention in the brain: A brief review of data and theories. Clin EEG Neurosci 37:330–335.

Vogeley K, Bussfeld P, Newen A, Herrmann S, Happe F, Falkai P, Maier W, Shah NJ, Fink GR, Zilles K (2001): Mind reading: Neural mechanisms of theory of mind and self-perspective. Neuroimage 14(1 Part 1):170–181.

Williams BR, Ponesse JS, Schachar RJ, Logan GD, Tannock R. (1999): Development of inhibitory control across the life span. Dev Psychol 35:205–213.

Worsley KJ, Marrett S, Neelin P, Vandal AC, Friston KJ, Evans AC (1996): A unified statistical approach for determining significant voxels in images of cerebral activation. Hum Brain Mapp 4:58–73.

Yeung N, Cohen JD, Botvinick MM (2004): The neural basis of error detection: Conflict monitoring and the error-related negativity. Psychol Rev 111:931–959.